Experimental verification of backward-wave radiation from a negative refractive index metamaterial

Anthony Grbic and George V. Eleftheriades[a]

The Edward S. Rogers Sr. Department of Electrical and Computer Engineering, University of Toronto,
10 King's College Road, Toronto, Ontario M5S 3G4, Canada

A composite medium consisting of an array of fine wires and split-ring resonators has been previously used to experimentally verify a negative index of refraction. We present a negative refractive index (NRI) metamaterial that goes beyond the original split-ring resonator/wire medium and is capable of supporting a backward cone of radiation. We report experimental results at microwave frequencies that demonstrate backward-wave radiation from a NRI metamaterial—a characteristic analogous to reversed Cherenkov radiation. The conception of this metamaterial is based on a fresh perspective regarding the operation of NRI metamaterials. © *2002 American Institute of Physics.* [DOI: 10.1063/1.1513194]

I. INTRODUCTION

The electromagnetic (EM) properties of a material can be described by its corresponding electric permittivity and magnetic permeability. These two parameters macroscopically describe the effects of induced electric and magnetic polarization.[1] The design of composite EM structures tailored to have specific macroscopic properties has been a research topic of interest for some time. Throughout the 1950s and 1960s, lattices of discrete obstacles or scatterers, termed "artificial dielectrics," were extensively studied.[2] These artificial dielectrics operate in the long wavelength regime where the wavelength of radiation is much longer than both scatterer dimension and periodic spacing. As a result, they can be considered as effective media when describing electromagnetic phenomena at a macroscopic level. The scatterers emulate the atoms or molecules in a dielectric and produce a net average polarization that gives rise to an effective permittivity. In general, the electromagnetic properties of such structures can be expressed in terms of an effective electric permittivity and magnetic permeability. A renewed interest in artificial dielectrics has emerged from recent advances in electromagnetic microstructures that have extended the range of achievable effective permittivity and permeability values. The burgeoning interest stems from the development of an effective medium that exhibits simultaneously negative values of permittivity and permeability.

The recent implementation of a microstructured material with negative magnetic permeability in the gigahertz range has quickly led to the development of a composite medium with simultaneously negative values of permeability and permittivity over a finite frequency range.[3–5] This composite medium has often been referred to as a negative refractive index (NRI) metamaterial. The reported metamaterial combines an array of metallic wires to attain negative effective permittivity with an array of split-ring resonators to achieve negative permeability. Its realization has launched a research area and renewed interest in EM phenomena associated with wave propagation in negative refractive index materials. In 1968, Veselago[6] theoretically investigated the electrodynamics of a medium with simultaneously negative values of permittivity and permeability. He termed these materials "left handed media" (LHM) since the wave-vector $\vec{k}$ forms a left-handed triplet with the vectors $\vec{E}$ and $\vec{H}$, the electric- and magnetic-field intensity. In such materials, phase velocity and energy flow are antiparallel, which results in counter-intuitive phenomena such as reversed refraction as well as reversals of the conventional Doppler shift and Cherenkov radiation. Subsequent work by Pendry proposed that flat slabs of negative refractive index metamaterial behave as unconventional lenses with interesting subwavelength resolving properties.[7]

Recent experiments by Shelby *et al.*[5] using the array of wires and split-ring resonators have demonstrated a left-handed propagation band and confirmed that LHMs do in fact exhibit reversed refraction as described by Veselago.[6] That is, a beam incident on a LHM from an ordinary right-handed medium (RHM) was shown to refract to the same side of the normal as the incident beam. In this article, we present a type of NRI metamaterial that goes beyond the original split-ring resonator/wire medium of[5] and is capable of supporting a backward cone of radiation. We report experimental results that demonstrate backward-wave radiation from a NRI metamaterial. The conception of this metamaterial is based on a fresh perspective regarding the operation of NRI metamaterials. This approach leads to structures that exhibit a negative refractive index over a large bandwidth. The cone of radiation emitted into free space by the NRI metamaterial is analogous to the reversed Cherenkov radiation predicted by Veselago.[6] The reported metamaterial supports reverse traveling EM waves with phase velocities greater than the speed of light and emits coherent backward-wave radiation much like that radiated from charged particles exceeding the speed of light in a LHM.

[a]Electronic address: gelefth@waves.utoronto.ca

(a)

(b)
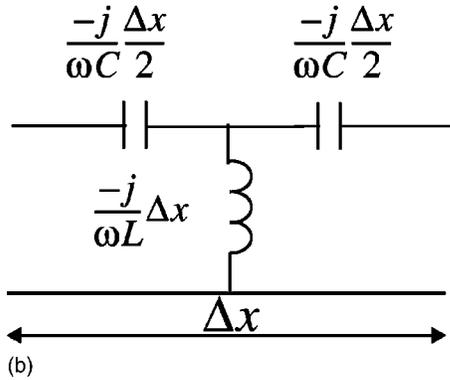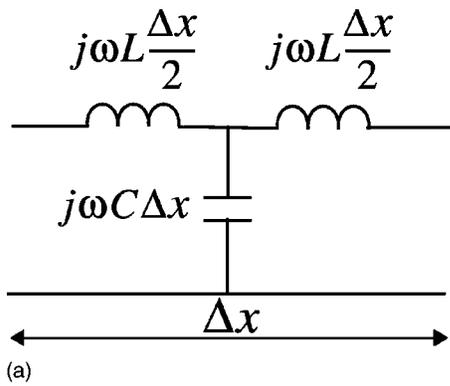
FIG. 1. Distributed transmission line representations. (a) Conventional TL. (b) Dual TL.

II. A PERSPECTIVE ON LHM OPERATION

The synthesis of the original split-ring resonator/wire NRI medium was based on separately considering an array of straight conducting wires to attain negative permittivity and an array of split-ring resonators to realize negative permeability.[4] Here, we take an approach, originating from the analogy that is readily drawn between transverse electromagnetic propagation on transmission lines (TLs) and plane-wave propagation in a homogeneous isotropic medium with positive material parameters, ϵ and μ. This equivalence forms the basis of the numerical technique called the transmission line modeling method.[8] Comparing the differential equations governing the propagation characteristics in both cases, the distributed L, C parameters of a conventional transmission line depicted in Fig. 1(a) can be related to the permittivity and permeability of the medium in the following manner:

$$\epsilon = C, \quad \mu = L. \tag{1}$$

This transmission line model of a medium with positive material parameters ϵ and μ itself offers insight into devising materials with negative ϵ and μ. Intuition would suggest that in order to synthesize a left-handed medium ($\epsilon < 0$ and $\mu < 0$), the series reactance and shunt susceptance shown in Fig. 1(a) should become negative, given that the material parameters are directly proportional to these circuit quantities. This change in sign implies the dual transmission line representation shown in Fig. 1(b) for synthesizing a medium with negative material parameters. Recently, slow-wave two-dimensional dual transmission line networks of this configu-
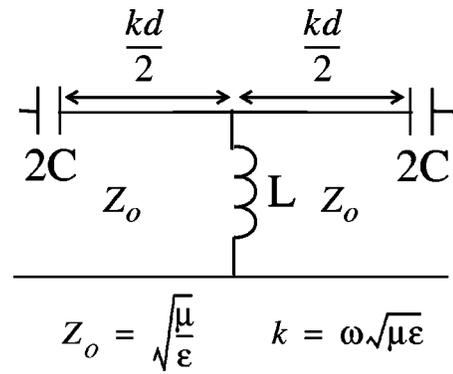
FIG. 2. A realizable dual transmission line structure.

ration have been used to demonstrate negative refraction and focusing of guided waves.[9] The dual transmission line structure can be implemented in practice by loading a host transmission line with lumped element series capacitors (C) and shunt inductors (L) as depicted in Fig. 2. In this periodic structure, the loading is strong such that the lumped elements dominate the propagation characteristics. For short interconnecting transmission line lengths ($kd \ll 1$, where k is the propagation constant of the interconnecting transmission lines and d is the unit-cell dimension) this periodic dual structure approaches the uniform dual structure shown in Fig. 1(b).

As for the conventional transmission line, analogous expressions for permittivity and permeability can be derived for Bloch waves guided by the dual structure shown in Fig. 2. Throughout the article, a time-harmonic variation of the form $e^{i\omega t}$ ($i = \sqrt{-1}$) is assumed. For electrically short interconnecting transmission line lengths ($kd \ll 1$) and small per-unit-cell phase delays ($\beta d \ll 1$, where β is the propagation constant of the Bloch waves guided by the periodic structure and d is the unit-cell dimension), the effective permittivity and permeability are given by the following approximate expressions:

$$\epsilon_{\mathrm{eff}} \approx \epsilon - \frac{1}{\omega^2 L d}, \tag{2}$$

$$\mu_{\mathrm{eff}} \approx \mu - \frac{1}{\omega^2 C d}, \tag{3}$$

where ω is the radial frequency and ϵ and μ represent the distributed capacitance and inductance of the short interconnecting transmission line sections acting as the host medium for this metamaterial. Equations (2) and (3) suggest that at high frequencies the effect of the loading reactances diminishes and the effective material parameters approach those of the unperturbed transmission line, ϵ and μ. In contrast, at low frequencies, the loading reactances dominate and the effective material parameters become negative for short interconnecting transmission lines

$$\epsilon_{\mathrm{eff}} \approx \frac{-1}{\omega^2 L d}, \quad \mu_{\mathrm{eff}} \approx \frac{-1}{\omega^2 C d}. \tag{4}$$

From an effective medium perspective, Eq. (2) indicates that the loading shunt inductors provide a negative electric sus-

ceptibility since they reduce the permittivity of the host medium (the interconnecting transmission line). As the value of the loading inductance is decreased, its effect becomes more pronounced and it eventually overcomes the permittivity of the host medium establishing a negative effective permittivity. Similarly, the series capacitor provides a negative magnetic susceptibility given that it reduces the permeability of the host medium. As the value of the capacitance is reduced, the negative magnetic susceptibility becomes more pronounced and eventually undermines the permeability of the host transmission line, causing the effective permeability to become negative.

Bloch analysis of the loaded dual transmission line structure yields the following expression for the Bloch propagation constant β:

$$\cos(\beta d) = \cos(kd)\left(1 - \frac{1}{4\omega^2 LC}\right)$$
$$+ \sin(kd)\left(\frac{1}{2\omega C Z_o} + \frac{Z_o}{2\omega L}\right) - \frac{1}{4\omega^2 LC}, \quad (5)$$

where Z_o $(\sqrt{\mu/\epsilon})$ represents the characteristic impedance and k $(\omega\sqrt{\mu\epsilon})$ the propagation constant of the interconnecting transmission line sections. For short interconnecting transmission line sections $(kd \ll 1)$ and small per-unit-cell phase delays $(\beta d \ll 1)$, the expression simplifies to

$$\beta \approx \pm \omega \sqrt{\left(\epsilon - \frac{1}{\omega^2 Ld}\right)\left(\mu - \frac{1}{\omega^2 Cd}\right)}, \quad (6)$$

which justifies Eqs. (2) and (3). This expression shows that the effect of the loading reactances diminishes as the frequency is increased and the propagation constant approaches that of the unperturbed transmission line, $\beta = \omega\sqrt{\mu\epsilon}$. On the other hand, for very short interconnecting transmission line sections or lower frequencies, the loading parameters govern the propagation characteristics. For this limiting case, simple circuit analysis shows that given positive power flow, the propagation constant β or equivalently the effective refractive index must be a negative quantity. The propagation constant and group velocity $(v_g = \partial\omega/\partial\beta)$ for the dual transmission line structure are approximately given by the following expressions:[10]

$$\beta \approx \frac{-1}{\omega\sqrt{LC}d}, \quad v_g \approx \omega^2 \sqrt{LC}d. \quad (7)$$

A negative propagation constant and a positive group velocity imply that energy flow and phase velocity are antiparallel (in this particular case, group velocity is parallel to the Poynting vector). Therefore, the structure supports backward waves and resembles a medium with a negative refractive index. These backward waves accumulate positive phase as they propagate away from their source. The expression for the propagation constant in Eq. (7) also indicates that a negative refractive index can be achieved over a large bandwidth if the periodicity d is chosen to be small. The approximate dispersion relations [Eqs. (6) and (7)] were derived for short interconnecting transmission line sections. The full dispersion relation [Eq. (5)] for representative transmission line
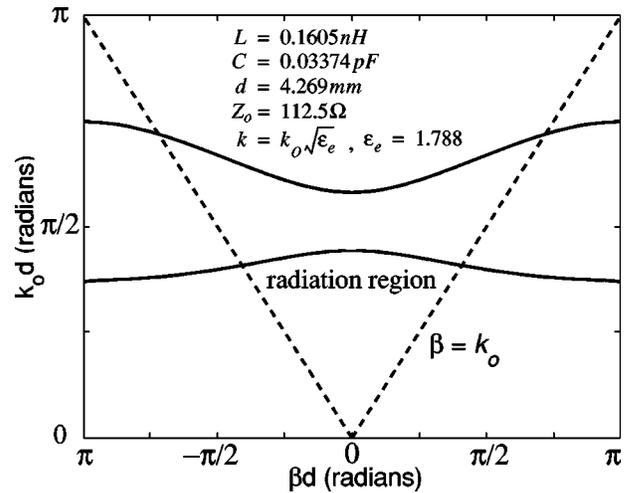
FIG. 3. Brillouin diagram for a realizable dual transmission line structure with representative TL and L, C loading parameters.

and L, C lumped element loading parameters is plotted in Fig. 3 in the form of a Brillouin diagram. Mutual impedance effects between neighboring cells are neglected and ideal transmission lines are assumed in this diagram. The variable k_o represents the propagation constant in free space ($k_o = \omega/c$, where c is the speed of light in a vacuum). As shown in Fig. 3, a stop band exists at low frequencies due to the high-pass configuration of the dual transmission line structure. This stop band extends from $\omega = 0$ to a cutoff frequency ω_c that can be approximated by the following expression:

$$\omega_c \approx \frac{1}{2\sqrt{LC}} \quad (8)$$

if the interconnecting transmission line sections are electrically short $(kd \ll 1)$.

Above this cutoff frequency, the phase velocity (ω/β) is negative for propagating waves with positive group velocities (i.e., positive slopes). Therefore, backward waves are supported in the lowest passband and the structure resembles a medium with negative refractive index. Above this lowest passband there exists another stop band. Within this stop band, the Bloch propagation constant remains an imaginary quantity. The lower stop band edge is caused by the effective permeability vanishing and the upper stop band edge results from the effective permittivity vanishing. These conditions can be easily understood from the approximate dispersion relation of Eq. (6).

III. BACKWARD-WAVE RADIATION

Charged particles traveling at speeds greater than the phase velocity of light in a medium emit coherent radiation better known as Cherenkov radiation. The angle of the radiated conical wave front is given by the velocity of the particle (V) with respect to the phase velocity of EM waves (v) within the medium in the following manner:

$$\cos\theta = \frac{v}{V} = \frac{c/n_o}{V}, \quad (9)$$

where n_o is the refractive index of the surrounding medium, c is the speed of light in a vacuum, and θ is the angle between the particle velocity and the radiated EM wave front. This expression suggests that in a medium with negative n_o, the angle θ becomes obtuse. This implies that radiation is directed backward rather than forward as is the case in a RHM.

Similarly, if a periodic guiding structure supports Bloch currents (moving charge) or equivalently EM waves with phase velocities greater than the speed of light, the angle of the radiated wave front is derived from Eq. (9) by letting V be the phase velocity of the EM wave along the guiding interface. This is due to the phase matching condition along the interface of the guide and surrounding medium. If the guiding structure is a medium with an effective refractive index n_1, and the surrounding medium has a refractive index n_o, then the angle of the radiated wave front is given by the following expression:

$$\cos \theta = \frac{c/n_0}{c/n_1} = \frac{n_1}{n_0}. \tag{10}$$

The above equation indicates that if the refractive index of the guiding medium (n_1) is negative, the radiation emitted into a RHM will be directed backward. It is in fact the phase advancement (backward-wave propagation) predicted by Eq. (7) that causes backward radiation into the surrounding medium.

In order to excite backward-wave radiation from the dual transmission line LHM into free space, the L, C parameters in Fig. 2 must be chosen such that the effective refractive index of the LHM, n_1, is negative and smaller in magnitude than one, as indicated by Eq. (10). Equivalently, the magnitude of the propagation constant along the guiding LHM, $|\beta|$ must be designed to be smaller in magnitude than the propagation constant in free-space k_o. This region of operation is identified on the Brillouin diagram in Fig. 3 as the radiation region.

IV. PROPOSED BACKWARD RADIATING STRUCTURE

The proposed implementation of a radiating NRI structure at 15 GHz based on the dual transmission line representation is shown in Fig. 4. The NRI antenna consists of 16 unit cells. It has a unit-cell dimension of 4.268 mm, approximately a factor of 5 smaller than the free-space wavelength of 2 cm at 15 GHz. Thus, the structure can be treated as an effective medium. The commercial method of moments software Agilent ADS (Advanced Design System) was used in designing the layout of the structure. The LHM was fabricated by a mask/photo-etching technique on a 20-mil thick Rogers RO3203 circuit board with a relative permittivity of 3. The interconnecting transmission line sections of Fig. 2 are implemented in coplanar waveguide (CPW) technology. The transmission lines consist of a planar center conductor with two adjacent ground planes on either side, as shown in Fig. 4. In the coplanar waveguide configuration, both ground planes and the center conductor lie in the same plane which allows the simple integration of shunt inductors and series capacitors. The gaps in the CPW center conductor serve as
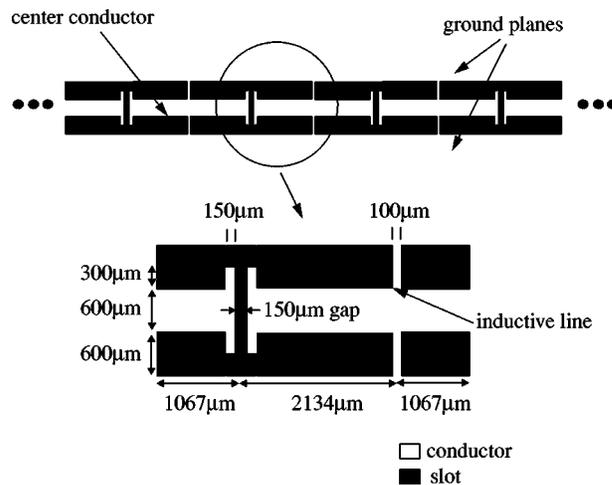
FIG. 4. Proposed backward-wave radiating metamaterial in coplanar waveguide at 15 GHz.

the series capacitors and the narrow lines connecting the center conductor to the coplanar ground planes act as the shunt inductors depicted in Fig. 2. It is in fact these capacitive gaps that radiate in the structure and cause a backward emerging transverse magnetic wave front. On the contrary, the inductive lines are nonradiating due to the antiparallel currents flowing on each pair of inductive lines. This odd symmetry causes cancellation in the far-field and leads to low cross-polarization levels.

Although there are various radiating structures that exhibit phase and group velocities of opposite sign, the proposed structure is the first to operate in the long wavelength regime and demonstrate backward-wave radiation in its lowest passband of operation. Indeed, as shown in Fig. 3, the proposed structure supports a backward-wave fundamental spatial harmonic that radiates. Early examples of backward-wave radiating structures include the helix antenna, corrugated dielectric, or metallic surfaces, and periodic arrays of radiating elements fed by slow wave transmission line sections of large periodic spacing ($d > \lambda/2$).[11,12] These structures, however, radiate in higher-order passbands (exhibit higher-order radiating spatial harmonics) and therefore effective material constants such as a refractive index cannot in general be defined. On the other hand, log-periodic dipole arrays and related uniform dipole arrays with a transposed feed have shown to produce backward waves even for small longitudinal periodic spacings.[13] Nevertheless, the dipoles are resonant so element dimensions still remain electrically large ($\approx \lambda/2$) and therefore effective material parameters, ϵ and μ cannot be defined either.

V. EXPERIMENTAL RESULTS

In the experiments, the proposed radiating NRI structure was used as a receiving antenna. It was rotated in $1°$ steps and illuminated by a transmitting horn antenna in an anechoic chamber 4.95 away in order to determine its far-field radiation patterns. The NRI antenna was connected to a vector network analyzer by a coaxial cable in order to measure the received power at the various illumination angles. A
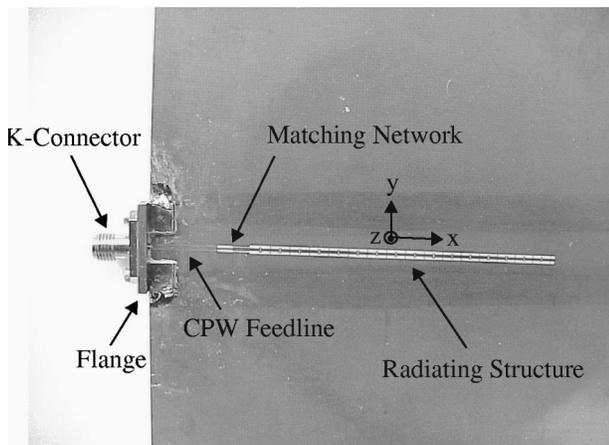
FIG. 5. Photograph of the backward-wave radiating metamaterial.

flange-mounted K-connector (coaxial) provided the transition from CPW feedline to the coaxial cable. A CPW impedance matching network consisting of two quarter wavelength transmission lines was incorporated at the input of the NRI antenna in order to minimize reflections at the input terminal. A photograph of the radiating structure along with the feedline, impedance matching network, and attached connector are shown in Fig. 5.

Figure 6 shows the principle planes of the NRI structure as well as the polarization of the illuminating E field at the angles θ and γ in the E plane and H plane, respectively. The proposed structure is located at the origin and runs along the x axis in Fig. 6. The normalized E plane and H plane radiation patterns are shown in Figs. 7(a) and 7(b). The angles θ and γ in Fig. 6 show how the angles in the E plane and H plane relate to the orientation of the NRI structure. A frequency shift of 400 MHz (3%) was observed in the measurements compared to the method of moments simulations. Therefore, the simulated patterns are given at 15 GHz and the measured patterns at 14.6 GHz. The measured E plane pattern clearly shows the formation of a backward cone of radiation. The main beam emerges backwards as is expected for NRI guided-wave structures in free space that posses an effective refractive index whose magnitude is less than one.
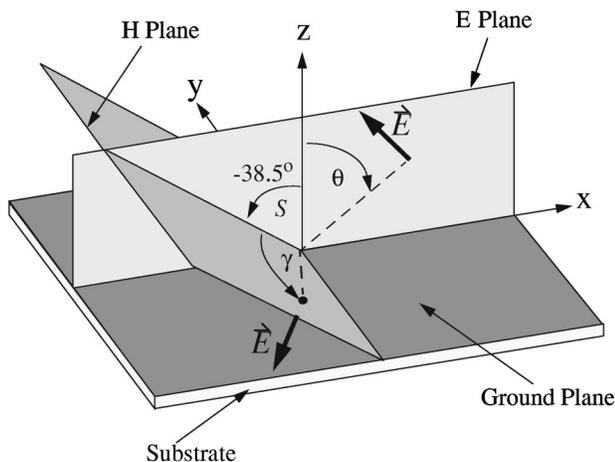
FIG. 6. Principle planes of the backward-wave radiating metamaterial.
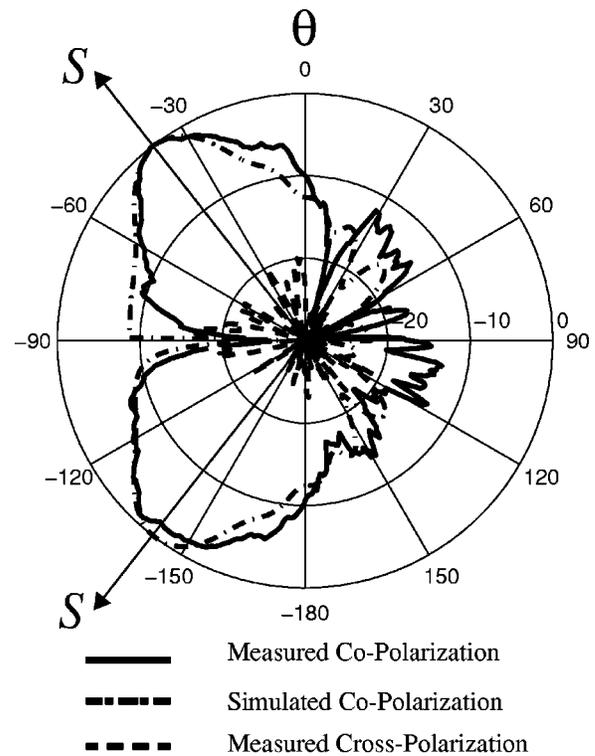
(a)
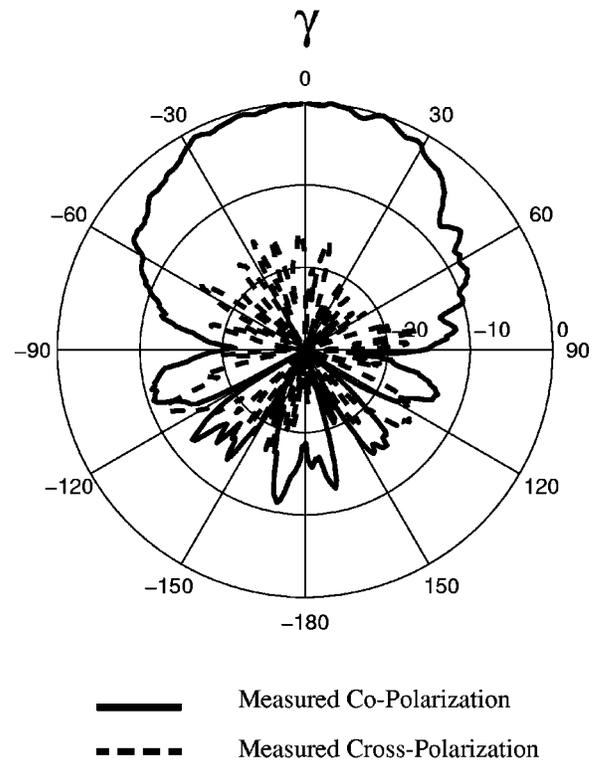
(b)

FIG. 7. Far-field patterns of backward-wave radiating metamaterial. (a) E plane far-field pattern. (b) H plane far-field pattern.

Specifically, the beam emerges at an elevation angle (S) of $\theta = -38.5°$ from broadside, which corresponds to a refractive index of -0.623 for the NRI antenna. The dispersive characteristics of the NRI antenna are evident both in simu-

lation and measurement. The radiated angle of emergence is frequency dependent as suggested by Eq. (7). With increasing frequency, the main beam scans away from the backfire direction toward the broadside direction [zero degrees in Fig. 7(a)].

VI. CONCLUSION

An approach to synthesizing NRI metameterials has been introduced. This approach based on the concept of dual transmission lines, leads to large bandwidths of NRI operation. In particular, a CPW-based NRI metamaterial was proposed that is capable of supporting backward radiation—a characteristic analogous to reversed Cherenkov radiation. Measurements have been reported demonstrating a backward radiating fundamental harmonic from a NRI metamaterial. Radiating metamaterials such as this exhibiting backward-wave propagation (phase propagation toward the source) open opportunities for developing planar, compact devices capable of beam steering, and microwave focusing. Applications may include wireless communications, surveillance, radar, and wireless power transmission. The dual transmission line representation on which the design of the metamaterial

rests may also motivate microwave devices that exploit the unique electromagnetic phenomena associated with left-handed media.

[1] E. C. Jordan and K. G. Balmain, *Electromagnetic Waves and Radiating Systems*, 2nd ed. (Prentice-Hall, Englewood Cliffs, NJ, 1968), Chap. 9.
[2] R. E. Collin, *Field Theory of Guided Waves*, 2nd ed. (IEEE Press, Piscataway, NJ, 1991), Chap. 12.
[3] M. C. K. Wiltshire *et al.*, Science **291**, 849 (2001).
[4] D. R. Smith *et al.*, Phys. Rev. Lett. **84**, 4184 (2000).
[5] R. A. Shelby, D. R. Smith, and S. Schultz, Science **292**, 77 (2001).
[6] V. G. Veselago, Usp. Fiz. Nauk **92**, 517 (1964) [Sov. Phys. Usp. **10**, 509 (1968).]
[7] J. B. Pendry, Phys. Rev. Lett. **85**, 3966 (2000).
[8] W. J. R. Hoefer, IEEE Trans. Microwave Theory Tech. **MTT-33**, 882 (1985).
[9] A. K. Iyer and G. V. Eleftheriades, in *IEEE MTT-S International Microwave Symposium Digest* (IEEE, Seattle, WA, 2002), Vol. 2, pp. 1067–1070.
[10] S. Ramo, J. R. Whinnery, and T. Van Duzer, *Fields and Waves in Communication Electronics*, 3rd ed. (Wiley, New York, 1994), Chap. 5.
[11] P. E. Mayes, Proc. IRE **49**, 962 (1961).
[12] R. E. Collin and F. J. Zucker, *Antenna Theory, Part II* (McGraw-Hill, New York, 1969), Chap. 19.
[13] P. G. Ingerson and P. E. Mayes, *Dispersion Properties of Linear Dipole Arrays*, Technical Report AFAL-TR-66-120, Department of Electrical Engineering, University of Illinois, 1966.